Hachimori, A., Matsumaga, A., Shimizu, M., Samejima, T., and Nosoh, T. (1974), *Biochim. Biophys. Acta 350,* 461-474.
Hubbard, J. S., and Stadtman, E. R. (1967a), *J. Bacteriol. 93,* 1045-1055.
Hubbard, J. S., and Stadtman, E. R. (1967b), *J. Bacteriol. 94,* 1016-1024.
Kingdon, H. S. (1974), *Arch. Biochem. Biophys. 163,* 429-431.
Ross, P. D., and Ginsburg, A. (1969), *Biochemistry 8,* 4690-4695.
Shapiro, B. M., and Stadtman, E. R. (1970), *Annu. Rev. Microbiol. 24,* 501-524.
Tate, S. S., and Meister, A. (1973), in The Enzymes of Glutamine Metabolism, Prusiner, S., and Stadtman, E. R., Ed., New York, N.Y., Academic Press, pp 77-128.
Tiemeier, D. C., Smotkin, D., and Milman, G. (1973), in The Enzymes of Glutamine Metabolism, Prusiner, S., and Stadtman, E. R., Ed., New York, N.Y., Academic Press, pp. 145-166.
Webb, J. L. (1963), Enzyme and Metabolic Inhibitors, Vol. I, New York, N.Y., Academic Press, p 49 ff.
Wedler, F. C. (1974), *Biochem. Biophys. Res. Commun. 60,* 737-742.
Wedler, F. C., and Boyer, P. D. (1972), *J. Theor. Biol. 38,* 539-558.
Wedler, F. C., and Hoffmann, F. M. (1974a), *Biochemistry 13,* 3207-3214.
Wedler, F. C., and Hoffmann, F. M. (1974b), *Biochemistry 13,* 3215-3221.
Wedler, F. C., Hoffmann, F. M., Kenney, R., and Carfi, J. (1976), *Experientia* (in press).
Woolfolk, C. A., Shapiro, B. M., and Stadtman, E. R. (1966), *Arch. Biochem. Biophys. 116,* 177-192.

Mechanistic Studies of Glutamine Synthetase from *Escherichia coli:* Kinetics of ADP and Orthophosphate Binding to the Unadenylylated Enzyme†

S. G. Rhee and P. B. Chock*

ABSTRACT: The kinetics of protein fluorescence change exhibited by ADP or orthophosphate addition to the Mg^{2+}- or Mn^{2+}-activated unadenylylated glutamine synthetase from *Escherichia coli* were studied. The kinetic patterns of these reactions are incompatible with a simple bimolecular binding process and a mechanism which required protein isomerization prior to substrate binding. They are consistent with a mechanism in which direct substrate binding is followed by a substrate-induced conformational change step, $ES \rightleftharpoons ES^*$. At pH 7.0 and 15 °C, the association constants for the direct binding (K_1) of ADP to $MnE_{1.0}$ and of P_i to $MnE_{1.0}ADP$ are 3.9×10^4 and 2.28×10^2 M^{-1}, respectively. The association constant for the direct binding of ADP to $MnE_{1.0}P_i$ is 2.3×10^4 M^{-1} at pH 7.0 and 19 °C. The $\Delta G°$ for the substrate-induced conformational step are -3.5 and -1.3 kcal mol^{-1} due to ADP binding to $MnE_{1.0}P_i$ and $MnE_{1.0}$, respectively, and -1.4 kcal mol^{-1} due to P_i binding to $MnE_{1.0}ADP$. Rate constants, k_2, and k_{-2}, for the isomerization step are: 90 and 9.5 s^{-1} for ADP binding to $MnE_{1.0}$, 440 and 0.36 s^{-1} for ADP binding to $MnE_{1.0}P_i$, and 216 and 1.8 s^{-1} for P_i binding to $MnE_{1.0}ADP$. Due to low substrate affinity, the association constant for direct P_i binding to $MnE_{1.0}$ was roughly estimated to be 230 M^{-1} and $k_2 = 750$ s^{-1}, $k_{-2} = 250$ s^{-1}. At 9 °C and pH 7.0, the estimated association constants for the direct ADP binding to $MgE_{1.0}$ and $MgE_{1.0}P_i$ are 1.8×10^4 and 1.6×10^4 M^{-1}, respectively; and the rate constants for the isomerization step associated with the corresponding reaction are $k_2 = 550$ s^{-1}, $k_{-2} = 500$ s^{-1}, and $k_2 = 210$ s^{-1}, $k_{-2} = 100$ s^{-1}. From the kinetic analysis it is evident that the inability of Mn^{2+} to support biosynthetic activity of the unadenylylated enzyme is due to the slow rate of ADP release from the $MnE_{1.0}P_iADP$ complex. In contrast the large k_{-2} obtained for ADP release from the $MgE_{1.0}ADP$ or $MgE_{1.0}P_iADP$ complex indicates that this step is not rate limiting in the biosynthesis of glutamine since the k catalysis obtained under the same conditions is 7.2 s^{-1}.

Glutamine synthetase, a key enzyme in nitrogen metabolism (Stadtman, 1973), has been extensively studied in recent years (Rhee et al., 1976; Stadtman and Ginsburg, 1974; Meister, 1974). The enzyme from *E. coli* is composed of 12 identical subunits (Woolfolk et al., 1966) and is regulated primarily by cascade control of the adenylylation and deadenylylation of a tyrosine residue in each subunit (Adler et al., 1974; Holzer, 1969; Shapiro et al., 1967). This enzyme is known to catalyze several reactions involving the conversion of glutamate to glutamine, or vice versa, glutamate or glutamine to γ-glutamyl hydroxamate and glutamate to pyrrolidonecarboxylate (Rhee et al., 1976; Stadtman and Ginsburg, 1974). Of these reactions, the biosynthetic and transferase reactions (reaction 1 and 2, respectively) are the most widely studied

† From the Laboratory of Biochemistry, Section on Enzymes, National Heart and Lung Institute, National Institutes of Health, Bethesda, Maryland 20014. *Received September 18, 1975.* This paper is Part III of a series on mechanistic studies of this enzyme. For Part II, see Rhee, S. G., Chock, P. B., and Stadtman, E. R. (1976), *Biochimie* (in press).

$$\text{L-glutamate} + \text{ATP} + \text{NH}_3 \overset{Me^{2+}}{\rightleftharpoons} \text{L-glutamine} + \text{ADP} + \text{P}_i \quad (1)$$

$$\text{L-glutamine} + \text{NH}_2\text{OH} \overset{Me^{2+}}{\underset{\text{ADP, P}_i \text{ or arsenate}}{\rightleftharpoons}} \gamma\text{-glutamyl hydroxamate} + \text{NH}_3 \quad (2)$$

(where Me^{2+} is divalent metal ion). Mg^{2+} will support catalysis of both reactions by the unadenylylated enzyme but it can not support any activity of the adenylylated enzyme. However, Mn^{2+} can support both catalytic activities of the adenylylated enzyme and the transferase activity of the unadenylylated enzyme but it will not support biosynthetic activity of the unadenylylated enzymes. Although forward biosynthetic activity with the Mn^{2+}-unadenylylated enzyme could not be detected by the conventional assay methods, we have shown (Rhee et al., 1976) that Mn^{2+}-unadenylylated enzyme catalyzes the reverse biosynthetic reaction, the glutamate dependent transfer of the γ-phosphoryl group of ATP to GDP, and the conversion of glutamate to pyrrolidonecarboxylate. In addition, our fluorescence studies suggest that conversion of glutamate to an activation complex (or complexes) is formed upon addition of ATP and L-glutamate to the unadenylylated enzyme in the presence of either Mg^{2+} or Mn^{2+}. Recently Wedler (Wedler, 1974) suggested that the release of ADP from the $MgE_{1.7}$[1] is the rate-limiting step for the biosynthetic reaction based on the relative rates of equilibrium isotopic exchange which showed that the ADP $\rightleftarrows$ ATP exchange rate is slower than the glutamate $\rightleftarrows$ glutamine and glutamine $\rightleftarrows$ NH_3 exchanges. In addition, it is known that ADP and orthophosphate or arsenate exhibit a strong synergistic effect with respect to their binding affinity for the Mn^{2+}-activated unadenylylated enzyme (Timmons et al., 1974a,b; Hunt et al., 1975). This synergistic effect can be achieved by increasing the association rate constants of ADP and orthophosphate with the enzyme or by decreasing their dissociation rate constants, likely through ligand induced protein conformational change.

In the present paper, we report the results of the stopped-flow kinetic studies on the binding of ADP and orthophosphate to the Mg^{2+}- and Mn^{2+}-activated unadenylylated enzyme. From a consideration of the rate constants for the binding of ADP and orthophosphate and the ligand induced conformational change steps involved, a mechanism is proposed to explain the observed results.

Experimental Section

Materials. The unadenylylated glutamine synthetase was isolated using the procedure developed by Woolfolk et al. (1966) from *E. coli* grown in a medium containing 20 mM NH_4Cl or 35 mM L-glutamate and 0.67 M glycerol. The state of adenylylation of this enzyme was 1.0 as determined both by the spectrophotometric method and by the γ-glutamyltransferase assay (Shapiro and Stadtman, 1970). The specific activity of the purified enzyme as determined by a modified procedure developed by Ginsburg et al. (1970) was 130 at 37 °C which agrees well with the published values for the purified enzyme. The reagents, ATP, ADP, and L-glutamine, were obtained from Sigma Chemical Co.

Methods. Fluorescence measurements were made using a Hitachi Perkin-Elmer MPF-2A instrument equipped with a Hewlett-Packard 7004B X-Y recorder and a homemade voltage offset circuit. Constant temperature was maintained using thermostated cell holders and constant-temperature circulating baths. A Cary 17 spectrophotometer equipped with thermostated cell holder was used for absorption spectra measurements.

Unless it is specified, all fluorometric measurements were carried out at 20 °C and the stopped-flow measurements were performed at 15 °C for $MnE_{1.0}$ and 9 °C for $MgE_{1.0}$ system in order to slow down the reaction rate. All reactions were carried out in 50 mM Hepes[2]-KOH and 0.1 M KCl buffered solutions at pH 7.0. Special care was taken to remove trace amounts of ammonia in the enzyme (Timmons et al., 1974b). All solutions were prepared with deionized water which had been freshly redistilled under argon atmosphere.

Fluorescence emission spectra of the enzyme were recorded with an excitation wavelength of 300 nm to give an emission spectrum with a maximum at 336 nm. With this excitation wavelength, the emission observed can be ascribed solely to the tryptophan residues in the enzyme which contains three or four residues per subunit (Woolfolk et al., 1966).

For the stopped-flow measurements, the same solution, which contained all required reagents except enzyme and the particular ligand under investigation, was used to prepare the two pre-mixed solutions. The solutions were equilibrated at the reaction temperature in a constant-temperature bath followed by 10 more min of incubation in the stopped-flow reservoir syringes.

The stopped-flow apparatus used consists of a pneumatic driving system from an Aminco Morrow stopped-flow machine equipped with either an Aminco Morrow mixer and observation cell or a homemade fast mixing cell which has a dead time of ca. 500 μs (to be published elsewhere). Both cells were thermostated at the reaction temperature. The light source used is a Hanovia 200-W mercury–xenon arc lamp with a low ripple Kepco JQE power supply. The light beam was passed through a Bausch and Lomb grating monochromator with a slit width of 1 or 2 mm before it reached the observation cell. The 90 °C fluorescence emission light from the tryptophan residues was filtered with an interference filter (Corion Instrument Corporation) with maximum transmission (~15%) at 340 nm and a half peak bandwidth of 10 nm. An EMI 9558 QBS-20 photomultiplier tube was mounted closely to the observation chamber in order to maximize the solid angle subtended by the photon-sensitive surface. Signal current from the last dynode of the 9558 QB S-20 was amplified by an Intersil 8007 operational amplifier in a current to voltage configuration. This signal was then further amplified, offset, filtered, and recorded on a Tektronix WP1200 Digital Processing Oscilloscope where signal averaging, semilog plot, and computation of rate constants were carried out.

The curve-fitting calculations were carried out by the use of an interactive curve-fitting and graphic program, MLAB, developed at National Institutes of Health and running on a PDP-10 digital computer (Knott and Reece, 1971).

Treatment of Data

As observed by the stopped-flow technique, the rate of

[1] The subscript indicates the average number of adenylylated subunits per dodecamer.

[2] Abbreviation used: Hepes, *N*-2-hydroxyethylpiperazine-*N'*-2-ethanesulfonic acid.

fluorescence change due to the binding of ADP or orthophosphate to the enzyme can be treated as either a one-step or two-step binding reaction. The one-step reaction is

$$E + S \underset{k_{-1}}{\overset{k_1}{\rightleftharpoons}} ES \quad (3)$$

where ES is enzyme-substrate complex and k_1 and k_{-1} are forward and reverse rate constants, respectively. When $[S]_0 \gg [E]_0$ (total concentration of S and E added), the rate observed will correspond to a pseudo-first-order rate, with the observed rate constant as

$$k_{obsd} = k_1[S]_0 + k_{-1} \quad (4)$$

This mechanism predicts a linear relationship between k_{obsd} and $[S]_0$.

A two-step reaction mechanism can involve either a molecular rearrangement of ES complex (eq 5) or a protein isomerization step as described in eq 6.

$$E + S \underset{k_{-1}}{\overset{k_1}{\rightleftharpoons}} ES \underset{k_{-2}}{\overset{k_2}{\rightleftharpoons}} ES^* \quad (5)$$

$$E \underset{k_{-1}}{\overset{k_1}{\rightleftharpoons}} E^* + S \underset{k_{-2}}{\overset{k_2}{\rightleftharpoons}} E^*S \quad (6)$$

When $[S]_0 \gg [E]_0$, with steady-state assumption and the condition that [ES*] or [E*S] is 0 at $t = 0$, the pseudo-first-order rate constants for reactions 5 and 6 are given by eq 7 and 8, respectively.

$$k_{obsd} = \frac{k_1[S]_0(k_2 + k_{-2}) + k_{-1}k_{-2}}{k_1[S]_0 + k_{-1} + k_2} \quad (7)$$

$$k_{obsd} = \frac{k_1(k_2[S]_0 + k_{-2}) + k_{-1}k_{-2}}{k_1 + k_{-1} + k_2[S]_0} \quad (8)$$

If the substrate addition step in reaction 5 is a rapid equilibrium reaction such that $k_{-1} \gg k_2$, then eq 7 is converted to eq 9

$$k_{obsd} = \frac{k_2}{1 + (K_1[S]_0)^{-1}} + k_{-2} \quad (9)$$

where $K_1 = k_1/k_{-1}$. If the rapid equilibrium step for reaction 6 is the isomerization step, then

$$k_{obsd} = [(k_2[S]_0)/(1 + K_1^{-1})] + k_{-2} \quad (10)$$

which indicates that k_{obsd} is a linear function of $[S]_0$. Equations 7-9 indicate that, at very high $[S]_0$, k_{obsd} is substrate concentration independent, such that $k_{obsd} = k_2 + k_{-2}$ for reaction 5 and $k_{obsd} = k_1$ for reaction 6. If the same protein isomerization is required for different substrate binding, then k_{obsd} should be independent of these substrates used for reactions which followed the mechanism described by reaction 6. All the k_{obsd} reported here plateau at high substrate concentration and the maximum k_{obsd} is substrate dependent. These are consistent with eq 7 and 9. However, only eq 9 will result in a linear reciprocal plot.

The values of K_1, k_2, and k_{-2} were obtained from computer curve-fitting using an interactive curve-fitting and graphic program.

Results

Fluorescence Changes Induced by ADP and Orthophosphate. Figure 1 shows the relative fluorescence emission changes at 336 nm due to the addition of ADP and orthophosphate to the $MgE_{1.0}$ and $MnE_{1.0}$ at 20 °C, pH 7.0. The magnitude of the fluorescence change is substrate concentration dependent until saturation is achieved. The amplitudes shown in Figure 1 are obtained at substrate concentration at least eight times above its dissociation constant. The amount of fluorescence enhancement provoked by ADP and orthophosphate is dependent on the divalent metal ion presence. In the case of $MnE_{1.0}$, the amount of fluorescence increase due to either substrate depends on the sequence of addition; however, the total fluorescence enhancement due to ADP and orthophosphate binding was independent of the sequence of addition. For example, when ADP was added first, a 67% fluorescence increase was detected, but only 50% was observed when ADP was added after P_i. In the case of $MgE_{1.0}$, within experimental error, the fluorescence enhancement due to each substrate is independent of the sequence of addition. From the changes in fluorescence caused by increasing concentrations of ADP and P_i, the binding constants for these substrates were calculated from modified Scatchard plots (Timmons et al., 1974b) and are given in Table I.

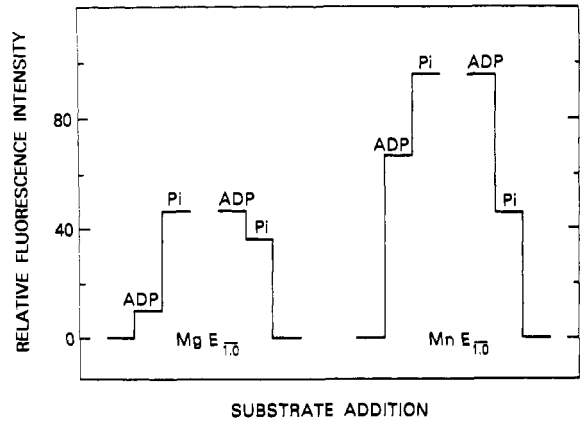

FIGURE 1: Relative protein fluorescence intensity enhanced by ADP addition followed by orthophosphate addition or vice versa for the $MgE_{1.0}$ and $MnE_{1.0}$. The reactions were carried out in 50 mM Hepes-KOH (pH 7.0) buffer containing 0.1 M KCl at 20 °C. The final concentrations for the Mg system are $[Mg^{2+}] = 20$ mM, [E] = 11 μM, [ADP] = 0.33 mM, $[P_i] = 40$ mM; for the Mn^{2+} system are $[Mn^{2+}] = 1$ mM, [E] = 11.6 μM, [ADP] = 0.2 mM, $[P_i] = 13$ mM. Excitation wavelength was 300 nm and emission was measured at 336 nm.

Table I: Dissociation Constants from Fluorometric Titration.[a]

	K_d (μM)
ADP + $MnE_{1.0}$	4.6 ± 1.5 (3.1)[b]
ADP + $MnE_{1.0}$Gln	2.4 ± 1.0
ADP + $MnE_{1.0}P_i$	0.05 ± 0.03(~0.02)[b,c]
P_i + $MnE_{1.0}$	1400 ± 300
P_i + $MnE_{1.0}$ADP	30 (±10)[c]
ADP + $MgE_{1.0}$	40[d] (±5)[c]
P_i + $MgE_{1.0}$	5000[d] ± 500
ADP + $MgE_{1.0}P_i$	30 (±10)[c]

[a] Unless it is specified, all data were obtained at pH 7.0, 20 °C, 50 mM Hepes-KOH buffer and 0.1 M KCl. The excitation wavelength was 300 nM and emission maximum was 336 nm. [b] pH 7.2, 25 °C (Hunt et al., 1975). [c] pH 7.6, 25 °C (Rhee et al., 1976). [d] pH 7.6, 25 °C.

Fast Kinetics of ADP and Orthophosphate Binding to Mg^{2+}- and Mn^{2+}-Supported $E_{1.0}$. The rates of fluorescence changes associated with the binding of ADP or orthophosphate to Mg^{2+}- or Mn^{2+}-supported unadenylylated enzyme were measured with a stopped-flow machine. The procedure and the apparatus used were described in the Experimental Section. The reactions were carried out in a 50

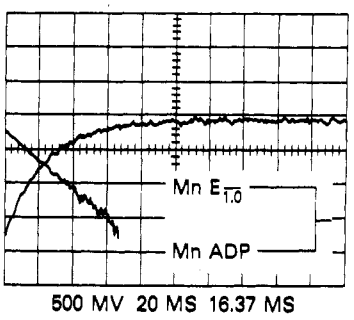

FIGURE 2: Oscilloscope tracing of protein fluorescence change for $MnE_{1.0}$ + MnADP reaction and the computer generated semilog plot for the corresponding curve. Final concentrations of reactants and buffer are $[MnE_{1.0}]$ = 1 μM, [MnADP] = 15 μM, [Hepes-KOH] = 50 mM, [KCl] = 0.1 M, $[Mn^{2+}]$ = 1 mM. The curve represents the fluorescence increase with 500 mV per division and the time scale is 20 ms per division. The straight line represents the plot of ln $(F_M - F_t)$ vs. time where F_M and F_t are fluorescence level at maximum and at time t, respectively. The vertical scale for the straight line is 1.3 per division. Excitation wavelength is 300 nm, emission at 336 nm.

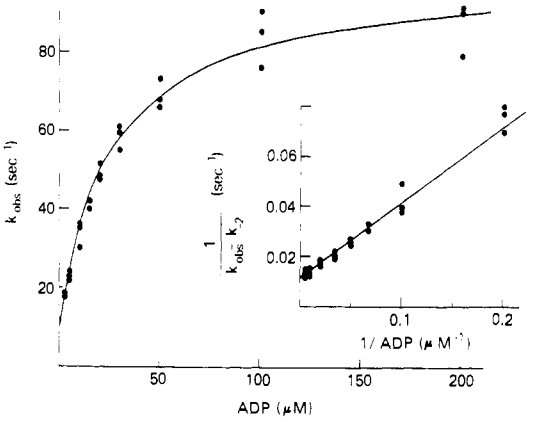

FIGURE 3: k_{obsd} for $MnE_{1.0}$ + ADP plotted as a function of ADP concentration. The curve is generated by computer simulation based on eq 9 to give $K_1 = 3.9 \times 10^4$ M^{-1}, $k_2 = 90$ s^{-1}, $k_{-2} = 9.5$ s^{-1}. The points are experimental values obtained at 15 °C, pH 7.0, 50 mM Hepes-KOH, 0.1 M KCl, 1 mM Mn^{2+}, 1 μM $E_{1.0}$, and [ADP] is a variable. The k_{obsd} for [ADP] $\leq$ 5 μM were derived from second-ordered rate constant measured. The insert is a plot of $(k_{obsd} - k_{-2})^{-1}$ vs. $[ADP]^{-1}$ for the same data.

mM Hepes buffer which containing 0.1 M KCl at pH 7.0. All the $MgE_{1.0}$ systems were measured at 9 °C while the $MnE_{1.0}$ systems at 15 °C, except for reaction 11 which was carried out at 19 °C to extend the range of P_i concentrations that could be used before precipitation of $Mn_3(PO_4)_2$ occurred. The reaction mixture was excited with 300-nm light and the fluorescence emission change with respect to time was recorded at 340 nm. The concentrations of enzyme or enzyme-substrate complex used for all reactions studied were in the range of 1–10 μM.

The reactions studied are:

$$MnADP + MnE_{1.0}P_i \quad (11)$$

$$MnADP + MnE_{1.0} \quad (12)$$

$$MnP_i + MnE_{1.0}ADP \quad (13)$$

$$MnP_i + MnE_{1.0} \quad (14)$$

$$MgADP + MgE_{1.0} \quad (15)$$

$$MgADP + MgE_{1.0}P_i \quad (16)$$

For reactions 11, 12, and 13, which are relatively slow (half-lives between 3 and 200 ms), an Aminco-Morrow mixer and observation cell were used. A typical oscilloscope tracing is shown in Figure 2. Pseudo-first-order rate constants, k_{obsd}, were calculated by the computer from these fluorescence enhancement curves and were plotted against the substrate concentrations, as shown in Figure 3. At low ADP concentrations, the k_{obsd} increases linearly with increasing ADP concentration and then plateaus at high ADP concentration. However, a plateau could not be demonstrated for the binding of P_i to $MnE_{1.0}ADP$ because $Mn_3(PO_4)_2$ precipitated at the higher P_i concentrations used. Nevertheless the k_{obsd} vs. $[P_i]$ plot is deviated from linearity when the concentration of P_i is higher than 1 mM. These data clearly show that k_{obsd} is not directly proportional to $[S]_0$; hence eq 4 can be rejected. For the same reason, a mechanism involving a rapid protein isomerization step as that described by reaction 6 can also be rejected since a linear function is required between k_{obsd} and $[S]_0$ (see eq 10). The results best fit a rate expression described by eq 9. A linear plot is obtained when $(k_{obsd} - k_{-2})^{-1}$ is plotted against $[S]_0^{-1}$ as shown in Figure 3. This is in accord with the rearrangement of eq 9. Computer-simulated curves based on eq 9 are given in Figure 3, and the rate constants so evaluated are tabulated in Table II.

The rates for reactions 14, 15, and 16 are too fast to measure with the Aminco-Morrow cell. A homemade fast mixer and observation cell which has a dead-time of 500 μs is used for these studies. A typical oscilloscope tracing is given in Figure 4. Since the dissociation constants for these reactions are relatively high and because their fluorescence changes are relatively small, the reactions are characterized by high rate and low amplitude; therefore, the rate constant determinations are subject to relatively large experimental errors. With this situation an accurate intercept at the k_{obsd} axis cannot be obtained (see Figure 5). However, the kinetic pattern shown in Figure 5 is clearly the same as that shown in Figure 3. The rate constants can be estimated and are given in Table II. For the purpose of comparison, the results of ADP binding to $MgE_{1.0}$ and $MgE_{1.0}P_i$ are shown in Figure 5.

Discussion

The kinetic data presented above show that binding of ADP or orthophosphate to either Mg^{2+}- or Mn^{2+}-activated enzyme or the enzyme-substrate complex is incompatible with a simple bimolecular association process. The data require at least a two-step reaction processes as described in eq 5 and 6. However, as described in the Treatment of Data section, all rate expressions derived from reaction 6 (eq 8 and 10) are inconsistent with the data obtained here, whether steady-state or rapid equilibrium mechanisms are assumed. Equation 8 indicates that at very high $[S]_0$, k_{obsd} is substrate concentration independent such that $k_{obsd} = k_1$. If the same protein isomerization is required for different substrate binding, then the maximum value of k_{obsd} obtained should be independent of these substrates used. This is clearly not the case being observed here. Equation 10 indicates that k_{obsd} is a linear function of $[S]_0$ which is inconsistent with the data. Therefore, a mechanism in which protein isomerization occurs prior to substrate addition need not be considered. Rate expressions for alternative mechanisms involving a substrate induced protein conformational change (reaction 5) are given by eq 7 and 9. The experimental data such as those shown in Figures 3 and 5

Table II: Kinetic Constants for the Two-Step Binding Mechanism.[a]

	Temp (°C)	K_1 (M^{-1})	k_2 (s^{-1})	k_{-2} (s^{-1})	K_d (M), kinetics[b]	K_d (M), titration[c]
ADP + $MnE_{1.0}$	15	$(3.9 \pm 0.36) \times 10^4$	90 ± 2	9.5 ± 1.5	$(2.7 \pm 0.6) \times 10^{-6}$	$(4.6 \pm 1.5) \times 10^{-6}$
ADP + $MnE_{1.0}P_i$	19	$(2.3 \pm 0.6) \times 10^4$	440 ± 72	0.36 ± 0.3	$(3.4 \pm 3) \times 10^{-8}$	$(5 \pm 3) \times 10^{-8}$
P_i + $MnE_{1.0}$ADP	15	228 ± 21	216 ± 29	1.8 ± 0.75	$(4 \pm 2) \times 10^{-5}$	$(3 \pm 1) \times 10^{-5}$
P_i + $MnE_{1.0}$	15	$(230)^d$	$(750)^d$	$(250)^d$	$(1.5 \times 10^{-3})^d$	$(1.4 \pm 0.5) \times 10^{-3}$
ADP + $MgE_{1.0}$	9	$(1.8 \times 10^4)^d$	$(550)^d$	$(500)^d$	$(3.7 \times 10^{-5})^d$	$(4 \pm 0.5) \times 10^{-5}$
ADP + $MgE_{1.0}P_i$	9	$(1.6 \times 10^4)^d$	$(210)^d$	$(100)^d$	$(3 \times 10^{-5})^d$	$(3 \pm 1) \times 10^{-5}$

[a] Kinetic constants obtained at pH 7.0, Hepes-KOH buffer (50 mM) and 0.1 M KCl. The constants are calculated based on eq 9. [b] Calculated from kinetic data, e.g., $K_d = k_{-2}/(K_1 k_2)$. [c] Constants from titration at pH 7.0, 20 °C except for the two $MgE_{1.0}$ systems which are obtained at pH 7.6, 25 °C. [d] Estimated value.

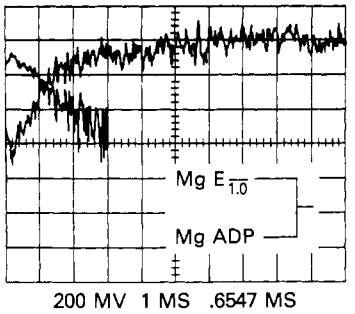

FIGURE 4: Oscilloscope tracing of protein fluorescence change when $MgE_{1.0}$ was mixed with MgADP in the stopped-flow with a homemade mixing chamber. The final concentration of each component is [$E_{1.0}$] = 10 μM, [ADP] = 0.5 mM, [Hepes-KOH] = 50 mM, [KCl] = 0.1 M, [Mg^{2+}] = 20 mM. The reaction was carried out at pH 7.0, 9 °C. The curve represents the fluorescence increase with 200 mV per division and the time scale is 1 ms per division. The straight line represents the semilog plog of the fluorescence change with respect to time produced by the computer. The vertical scale for the semilog plot is 1.1 per division. The excitation wavelength is 300 nm, emission at 366 nm.

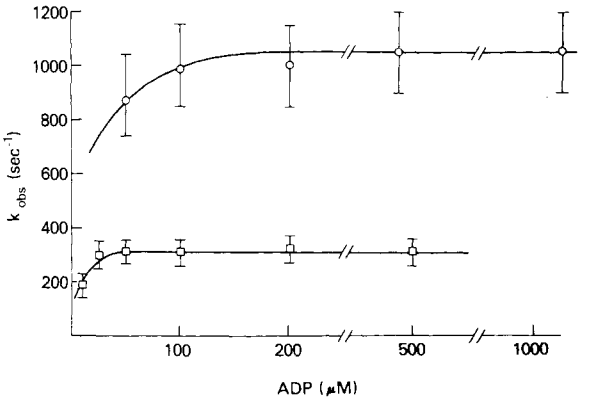

FIGURE 5: The dependent of k_{obsd} on ADP concentration for ADP binding to $MgE_{1.0}$ (○) and $MgE_{1.0}P_i$ (□). In this experiment [Hepes-KOH] = 50 mM, [KCl] = 0.1 M, [Mg^{2+}] = 20 mM, [$E_{1.0}$] = 10 μM, [P_i] = 25 mM for (□), and [ADP] is a variable. The reaction was carrried out at pH 7.0, 9 °C.

are best explained by eq 9. Accordingly, the data are consistent with the mechanism depicted by reaction 5 in which $k_{-1} \gg k_2$. This indicates that the first step is in rapid equilibrium. Assuming this mechanism is correct, by using eq 9, the values of k_2, k_{-2}, and K_1 were calculated for ADP binding to $MnE_{1.0}$ and $MnE_{1.0}P_i$, and for orthophosphate binding to $MnE_{1.0}$ADP, respectively, and are reported in Table II. The value for k_1 was estimated with the assumption that ES is a collision intermediate, which is formed at a diffusion-controlled rate $\sim 10^8$ M^{-1} s^{-1} (Eigen and Hammes, 1963). It follows that k_{-1} is 2×10^3, 2.6×10^3, and 4.4×10^5 s^{-1} for ADP binding to $MnE_{1.0}P_i$, $MnE_{1.0}$ and for orthophosphate binding to $MnE_{1.0}$ADP, respectively. Since fluorescence of ES should be the same as that of E, the observed fluorescence change must be due to substrate-induced isomerization of the enzyme. This is supported by the fact that no biphasic phenomenon is observed and the amplitude is proportional to $[S]_0$ till saturation is reached. The $\Delta G°$ values for the substrate-induced conformational change step, ES ⇌ ES*, are −3.5 and −1.3 kcal mol^{-1} for ADP binding to $MnE_{1.0}P_i$ and $MnE_{1.0}$, respectively. When orthophosphate binds to $MnE_{1.0}$ADP, a $\Delta G°$ of −1.4 kcal mol^{-1} was obtained for the substrate-induced conformational change process. Unfortunately, one cannot evaluate the $\Delta G°$ for the substrate-induced step for the ADP binding to $MgE_{1.0}$ or $MgE_{1.0}P_i$, nor for the binding of orthophosphate to $MnE_{1.0}$ because the relatively high error involved in determination of the rate constants makes it impossible to obtain an accurate intercept (see Figure 5). However, the value of $k_2 + k_{-2}$ for each case can be estimated. They are 1000, 350, and 1000 s^{-1} for ADP addition to $MgE_{1.0}$, $MgE_{1.0}P_i$, and for orthophosphate binding to $MnE_{1.0}$, respectively.

The data in Table II indicate that in the binding of ADP to $MnE_{1.0}$ orthophosphate increases the value of $k_2 + k_{-2}$ from 99.5 to 440 s^{-1}. To achieve this, it increases k_2 from 90 to 440 s^{-1} and decreases k_{-2} from 9.5 to 0.36 s^{-1}. In contrast, orthophosphate decreases the value of $k_2 + k_{-2}$ for ADP binding to $MgE_{1.0}$ from 1050 to 310 s^{-1} (Figure 5). Extrapolation of the $MgE_{1.0}$ curve in Figure 5 gives an approximate intercept of 500 s^{-1} (k_{-2}). This value is in reasonable agreement with the fact that, in the absence of orthophosphate, ADP does not affect the binding rate of ATP. In addition, we have observed that k_{obsd} (140 s^{-1} at pH 7.0 and 15 °C) for the fluorescence enhancement due to the addition of ATP (5 mM) to the $MgE_{1.0}GluNH_3$ ([Glu] = 50 mM, [NH_3] = 50 mM) complex is the same as that obtained for the addition of ATP to the $MgE_{1.0}$GluNH_3ADP ([Glu] = 50 mM, [NH_3] = 50 mM, [ADP] = 0.25 mM) complex. The only difference is that the reaction amplitude observed in the presence of ADP is about 80% of that observed when no ADP is present (Rhee, unpublished data). This lower amplitude is due to initial fluorescence contribution of ADP-enzyme complex. With the assumption that k_{-2} = 500 s^{-1}, k_2 and K_1 can be evaluated to be 550 s^{-1} and 1.8×10^4 M^{-1}, respectively. The value of K_1 is in the same order of magnitude as those obtained for ADP

binding to $MnE_{1.0}$ in the presence or absence of orthophosphate. If a similar K_1 is associated with the binding of ADP to $MgE_{1.0}P_i$, then the corresponding k_{-2} value should be equal to or greater than 100 s^{-1}. All the k_{-2} values estimated for the reactions of ADP with $MgE_{1.0}$ indicate that ADP release cannot be the rate-limiting step in the biosynthetic reaction where the k_c (catalysis) is 7.2 s^{-1} under the same conditions at 15 °C. However, k_{-2} for the release of ADP from $MnE_{1.0}P_iADP$ is 0.36 s^{-1}, which is clearly very slow relative to k_c observed for the Mg^{2+} activated enzyme. From the fact that $k_2 + k_{-2} = 1000$ s^{-1} and with the assumption that K_1 for the binding of P_i to $MnE_{1.0}$ is the same as that ($K_1 = 230$ M^{-1}) for the binding of P_i to $MnE_{1.0}ADP$, k_2 and k_{-2} for orthophosphate binding to $MnE_{1.0}$ can be evaluated to be 750 and 250 s^{-1}, respectively.

The fact that K_d calculated from the kinetic constants are in good agreement with the K_d determined by fluorescence titration (Table II) provides further support for the substrate-induced protein conformational change mechanism. In addition, the data in Table I indicate that with the Mn^{2+}-activated enzymes the effects of ADP and P_i are strongly synergistic, but less pronounced effects are obtained with the Mg^{2+}-activated enzyme. With $MnE_{1.0}$, L-glutamine also enhances the binding of ADP by a factor of 2. These synergistic effects suggest that either a substrate-induced conformational change or a direct substrate–substrate interaction is involved. Since the K_1 for ADP binding to $MnE_{1.0}$ is about the same as that for ADP binding to $MnE_{1.0}P_i$, the synergistic effects must be attributed to difference in the ratio of k_{-2} to k_2. This may suggest that the P_i induced protein conformation does not enhance the initial binding affinity of ADP. Rather, it is the result of a direct ADP–P_i interaction which enhances the apparent binding affinity of ADP and P_i.

In conclusion, we have demonstrated that a two-step substrate binding mechanism is required to explain the kinetic data of ADP and P_i binding to either the Mg^{2+}- or Mn^{2+}-supported unadenylylated enzyme. The first step is a direct substrate binding to the enzyme followed by a substrate-induced or a substrate–substrate-complex-induced protein isomerization step. It is believed that the result of this isomerization is responsible, at least in part, for the synergistic effect exhibited by substrate binding. Further, the data also show that the release of ADP from $MgE_{1.0}ADP$ or $MgE_{1.0}ADPP_i$ is not the rate-limiting step for the biosynthetic reaction. In contrast the slow rate of ADP release from $MnE_{1.0}ADPP_i$ may explain the inability to detect biosynthetic activity with $MnE_{1.0}$ by means of conventional assay methods.

Acknowledgment

The authors thank Dr. E. R. Stadtman for valuable discussions during the course of this work and helpful comments on the manuscript.

References

Adler, S. P., Mangum, J. H., Magni, G., and Stadtman, E. R. (1974), in Third International Symposium on Metabolic Interconversion of Enzymes, Fisher, E. H., Krebs, E. G., and Stadtman, E. R., Ed., New York, N.Y., Springer-Verlag, pp 221–233.

Eigen, M., and Hammes, G. G. (1963), *Adv. Enzymol. 25,* 1–38.

Ginsburg, A., Yeh, J., Hennig, S. B., and Denton, M. D. (1970), *Biochemistry 9,* 633–648.

Holzer, H. (1969), *Adv. Enzymol. 32,* 297–326.

Hunt, J. B., Smyrniotis, P. Z., Ginsburg, A., and Stadtman, E. R. (1975), *Arch. Biochem. Biophys. 166,* 102–124.

Knott, G. D., and Reece, D. K. (1971), Modellab Users Documentation, Division of Computer Research and Technology Report, September 1971, Bethesda, Md., National Institutes of Health.

Meister, A. (1974), *Enzymes, 3rd Ed. 10,* 699–754.

Rhee, S. G., Chock, P. B., and Stadtman, E. R. (1976), *Biochimie* (in press).

Shapiro, B. M., Kingdon, H. S., and Stadtman, E. R. (1967), *Proc. Natl. Acad. Sci. U.S.A. 58,* 642–649.

Shapiro, B. M., and Stadtman, E. R. (1970), *Methods Enzymol. 17A,* 910–922.

Stadtman, E. R. (1973), in The Enzymes of Glutamine Metabolism, Prusiner, S., and Stadtman, E. R., Ed., New York, N.Y., Academic Press, pp 1–6.

Stadtman, E. R., and Ginsburg, A. (1974), *Enzymes, 3rd Ed. 10,* 755–807.

Timmons, R. B., Huang, C. Y., Stadtman, E. R., and Chock, P. B. (1974a), in Metabolic Interconversion of Enzyme, Fisher, E. H., Krebs, E. G., Neurath, H., and Stadtman, E. R., Ed., Berlin, Springer-Verlag, pp 209–220.

Timmons, R. B. Rhee, S. G., Luterman, D. L., and Chock, P. B. (1974b), *Biochemistry 13,* 4479–4485.

Wedler, F. C. (1974), *J. Biol. Chem. 249,* 5080–5087.

Woolfolk, C. A., Shapiro, B. M., and Stadtman, E. R. (1966), *Arch. Biochem. Biophys. 116,* 177–192.